I&EC research
Industrial & Engineering Chemistry Research

Article

pubs.acs.org/IECR

Metal-Modified Cu-BTC Acid for Highly Enhanced Adsorption of Organosulfur Species

Hui Sun,*[,†] Xiao Han,[†] Kefeng Liu,[†] Benxian Shen,[†] Jichang Liu,[†] Di Wu,[‡,§,∥] and Xiaoyu Shi[†]

[†]Petroleum Processing Research Center, East China University of Science and Technology, Shanghai 200237, China
[‡]The Gene and Linda Voiland School of Chemical Engineering and Bioengineering, [§]Department of Chemistry, and [∥]Materials Science and Engineering, Washington State University, Pullman, Washington 99163, United States

Supporting Information

ABSTRACT: In this study, we provide an approach to the tunable metal modification on Cu-BTC (BTC= 1,3,5-benzenetricarboxylic acid) in order to achieve a highly enhanced adsorption affinity toward organosulfur species. We propose a strategy to regulate the metal compositions via the well-controlled reduction of Cu(II) to Cu(I) in Cu-BTC using ethanol as the reducing agent coupled with loaded Ag as catalyst under mild conditions. Applying scanning electron microscopy (SEM), energy-dispersive spectrometry (EDS), powder X-ray diffraction (XRD), Fourier transform infrared spectroscopy (FTIR), Raman spectroscopy, and X-ray photoelectron spectroscopy (XPS), we confirmed the successful modification and explored their structural changes. The quantitative relationship between metal compositions of Cu-BTC samples and their adsorption capacities for organosulfur compounds including dimethyl disulfide (DMDS), ethyl sulfide, and 1-propanethiol were highlighted, and the underlying adsorption mechanism was elucidated. Present results have significant implications for the optimal design and manipulation of the compositions as well as structures of metal−organic porous materials for adsorption desulfurization and better understanding of the role of metal species in sulfide adsorption.

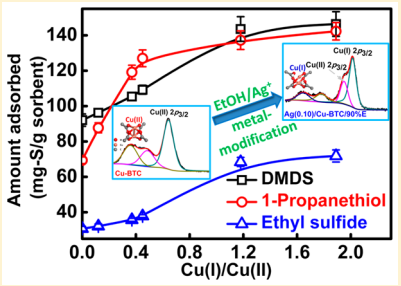

INTRODUCTION

Fossil fuels including gasoline, kerosene, diesel, liquefied petroleum gas (LPG), and natural gas (NG) have been widely used in residential, commercial, and transportation applications for tens of years. However, when using these fuels, one of the most important issues is the effective removal of their impurities, especially concerning small organosulfur compounds, such as mercaptans, thioethers, disulfides, and others.[1] These compounds and their sulfur oxides (SO_x) upon combustion are not only hazardous to human health and environment, but also harmful to the catalysts involved in various catalytic processes which convert hydrocarbons to more valuable products.[2,3] In recent years, reducing the sulfur content in fuels has become a growing environmental concern because of the constantly updated emission regulations. Thus, many efforts have been dedicated to achieving this purpose.

A number of new technologies based on selective adsorption,[4,5] biological treatment,[6] and extraction[7,8] have been proposed. Among these methods, adsorption desulfurization (ADS) is considered to be one of the most promising methods to overcome the limitations with the traditional hydrodesulfurization (HDS) process.[9−11] A wide range of porous solid adsorbents including ion-exchanged zeolites,[12−14] carbon-based materials,[15−17] and mesoporous aluminosilicates,[18] as well as metal oxides,[19,20] have been developed and investigated. Metal−organic frameworks (MOFs) are more versatile for application-oriented tailoring than other materials because of their ultrahigh surface areas, unique pore structures, modifiable pore dimensions, and chemical tunability.[21] Such characteristics are in theory able to make them promising candidates for potential applications in adsorption, separation, gas storage, and catalysis.[22−25] Specifically, exploration of the applications of MOFs has been confined to removing toxic or environmentally hazardous compounds from industrial waste gases.[26,27] Magnificent progresses have been successfully designed for adsorption desulfurization via the use of a variety of MOF structures including MOF-5, MOF-177, MOF-199, MOF-505, and UMCM-150.[28]

It has been found that MOFs with coordinatively unsaturated sites (CUSs, or open metal sites),[29,30] such as Cu-BTC (BTC = 1,3,5-benzenetricarboxylic acid) and MOF-74(Ni), are potential structures for preferential adsorption affinity toward organosulfur compounds. Specifically, Cu-BTC shows the highest adsorption capacity of organosulfur compounds.[31,32] According to Pearson's hard and soft acid−base theory, the sulfur-containing compounds (acting as soft bases) are strongly attracted to the metal sites such as Cu(II), Cu(I), and Ag (playing a role of soft Lewis acid). Besides, π-complexation is also considered as one of the most widely understood mechanisms for adsorption desulfurization. The d-block metals and their cations can interact with sulfur compound molecules

Received: June 10, 2017
Revised: August 4, 2017
Accepted: August 8, 2017
Published: August 8, 2017

DOI: 10.1021/acs.iecr.7b02392
Ind. Eng. Chem. Res. 2017, 56, 9541−9550

via π-complexation and adsorb them in facedown orientation on a flat surface, which helps achieve an excellent adsorption capability.[33] The most prominent metal ions for π-complexation are Cu(I) and Ag.[34,35]

A number of research studies have been done on the modification of MOFs in order to attain the improved performances for sulfur removal. Due to its tunable chemical structure, Cu-BTC has received wide interest in the structural modification. A remarkably high adsorption capacity for benzothiophene can be obtained by using phosphotungstic acid loaded Cu-BTC.[36] Szanyi et al. presented the extensive reduction/oxidation of copper moieties in the organic structure after coordinating CO or NO molecules.[37] Recent publications also reported the reduction of supported Cu(II) in several MOF structures by using different reducing agents including methanol, ethanol, formaldehyde, and hydroquinone.[38,39] However, the influences of metal compositions (referring to the host metals from the original framework as well as the migrant metals) on the adsorption desulfurization of Cu-BTC structures, though recognized as remarkable, have not been investigated in detail.

In the present work, we present an approach to metal modification on Cu-BTC in order to attain a highly enhanced adsorption affinity toward small organosulfur compounds. The reduction of Cu(II) to Cu(I) in the Cu-BTC framework was well-tuned via the controlled use of ethanol as reducing agent and impregnated Ag as catalyst under mild conditions. In addition, the quantitative relationship between metal composition and adsorption activity for small organosulfur compounds was highlighted. Furthermore, the mechanism for sulfur capture on the metal-modified Cu-BTC was also examined.

MATERIALS AND METHODS

Chemicals. $Cu(NO_3)_2{\cdot}3H_2O$ (with >99.0% purity) and 1,3,5-benzenetricarboxylic acid (BTC) (with >98.0% purity) were purchased from Shanghai Macklin Biochemical Co., Ltd. (Shanghai, China). *N*,*N*-Dimethylformamide (DMF) (with >99.5% purity), $AgNO_3$ (with >99.8% purity), and ethanol (with >99.5% purity) were provided by Shanghai Titan Scientific Co., Ltd. (Shanghai, China). Ethyl sulfide (with >97.0% purity) was provided by Adamas Reagent Co., Ltd. (Shanghai, China). Dimethyl disulfide (DMDS) (with >98.0% purity) and 1-propanethiol (with >98.0% purity) were purchased from Tokyo Chemical Industry Co., Ltd. (Tokyo, Japan). Deionized water was used in all cases. All the chemicals in this study were used as received.

Preparation of Samples. Cu-BTC was synthesized by using the solvothermal method reported previously.[36] At first, solutions I and II were prepared by dissolving 6 g of $Cu(NO_3)_2{\cdot}3H_2O$ into 40 mL of deionized water and 3 g of BTC into a mixture of 40 mL of ethanol and 40 mL of DMF, respectively. Then the two solutions were mixed and treated under ultrasound at 40 kHz and 120 W (JP-020S, Skymen Cleaning Equipment Shenzhen Co., Ltd., Shenzhen, China) for 10 min at room temperature. Hereafter, the mixture was transferred into a 150 mL stainless steel autoclave with a polytetrafluoroethylene liner and kept at 85 °C for 24 h. After cooling, the blue products were separated by centrifugation and washed using ethanol three times. The resulting Cu-BTC products were dried at 160 °C for 15 h.

The metal modification on Cu-BTC was carried out via the reduction of Cu(II) to Cu(I) in the EtOH−H_2O systems coupled with Ag loading. A certain amount of $AgNO_3$ was dissolved in EtOH−H_2O solution under 40 kHz ultrasound condition for 10 min at room temperature. The loading of Ag was done by the postsynthesis method. A 2 g sample of synthesized Cu-BTC was immersed in 100 mL of EtOH−H_2O solution (having $AgNO_3$ concentrations of 0−0.147 mol/L) in the previously mentioned stainless steel autoclave and kept at 85 °C for 20 h. Different solvent compositions (with the volume fractions of EtOH ranging from 0 to 100%) were used and the starting Ag/Cu molar ratios were changed from 0 up to 1.50. The resulting solids were washed at least three times using corresponding solvent and separated by centrifugation. After being dried at 160 °C for 10 h, the cyan solid products were obtained. All the samples were labeled as Ag(n)/Cu-BTC/solvent, where n is the starting Ag/Cu molar ratio used in the postsynthesis. Specially, the item of Ag(n) was omitted in the case of n = 0. As for the solvent item, "E" and "W" refer to EtOH and H_2O and v%E denotes the EtOH−H_2O solvent with the volume fraction of EtOH of v%.

Characterization. The morphologies of samples were analyzed by using a NOVA Nano SEM450 scanning electron microscope (SEM; FEI, USA) with a beam current of 10 nA and an accelerating voltage of 15 kV. Element analyses were carried out on a Falcon energy-dispersive spectrometer (EDS; EDAX Inc., USA). A sputter coating with a thin layer of platinum was performed to avoid charging. Five to eight points were measured at various positions to obtain an average elemental composition. Homogeneity was checked using backscattered electron (BSE) imaging.

The pore structure of Cu-BTC was determined by N_2 adsorption at 77 K using a 3H-2000PM2 automatic physisorption analyzer (BeiShiDe Instrument Co., Ltd., Beijing, China). The specific surface area was calculated using the Brunauer−Emmett−Teller (BET) method. The pore volume and average pore diameter were calculated using the Barrett−Joyner−Halenda (BJH) method.

Powder X-ray diffraction (XRD) patterns were collected at room temperature using a Rigaku D/max 2550 diffractometer (Rigaku Industrial Corp., Japan) using Cu Kα radiation operated at 18 kW and 450 mA. The 2θ scanning angle range was 5−75° with step sizes of 0.02 and 5 deg min^{-1}.

Fourier transform infrared spectroscopic (FTIR) analyses were carried out on a Nicolet 6700 FTIR spectrometer (Thermo Fisher Scientific, USA) using a KBr tablet. Each spectrum was obtained from the acquisition of 105 scans with a resolution of 2 cm^{-1} from 4000 to 400 cm^{-1}.

Raman spectra were obtained by using a Renishaw inVia Reflex Raman microscope and spectrometer (Renishaw Plc., U.K.) fitted with a 514 nm argon ion laser. Data were recorded from 4000 to 100 cm^{-1} with a spectral resolution of 1.14 cm^{-1} and using a grating of 2400 lines/mm.

Contents of Ag and Cu in the postsynthesis solutions were determined using a Varian 710-ES inductively coupled plasma atomic emission spectrometer (ICP-AES; Agilent Technologies, USA).

X-ray photoelectron spectroscopy (XPS) measurement was conducted with a Thermo Scientific ESCALAB 250Xi spectrometer (Thermo Fisher Scientific, USA) equipped with Al Kα radiation as the X-ray source (14 kV, 250 W). XPS spectra of the samples were corrected on the basis of the reference of carbon (C 1s, 284.6 eV). To further determine the valence of Cu in the structure of Cu-BTC, X-ray Auger electron spectroscopy (XAES) was also conducted in the Cu LMM region. The detailed information on the valence state of Cu

DOI: 10.1021/acs.iecr.7b02392
Ind. Eng. Chem. Res. 2017, 56, 9541−9550

Table 1. Chemical Compositions of Cu-BTC Samples

sample	experimental condition: solvent[a]	experimental condition: exptl n(Ag)/n(Cu)	chem composition[b]	obsd n(Ag)/n(Cu)
Cu-BTC	–	0	$Cu_3(BTC)_2$	0
Cu-BTC/E	100% EtOH	0	$Cu_3(BTC)_2$	0
Cu-BTC/50%E	50% EtOH + 50% H_2O	0	$Cu_3(BTC)_2$	0
Cu-BTC/90%E	90% EtOH + 10% H_2O	0	$Cu_3(BTC)_2$	0
Ag(0.10)/Cu-BTC/W	100% H_2O	1/10	$Ag_{0.01}Cu_{2.99}(BTC)_{1.99}$	0.02
Ag(0.10)/Cu-BTC/20%E	20% EtOH + 80% H_2O	1/10	$Ag_{0.04}Cu_{2.96}(BTC)_{1.97}$	0.07
Ag(0.02)/Cu-BTC/50%E	50% EtOH + 50% H_2O	1/50	$Ag_{0.006}Cu_{2.99}(BTC)_{1.99}$	0.01
Ag(0.03)/Cu-BTC/50%E	50% EtOH + 50% H_2O	1/30	$Ag_{0.01}Cu_{2.99}(BTC)_{1.99}$	0.02
Ag(0.05)/Cu-BTC/50%E	50% EtOH + 50% H_2O	1/20	$Ag_{0.02}Cu_{2.98}(BTC)_{1.98}$	0.04
Ag(0.10)/Cu-BTC/50%E	50% EtOH + 50% H_2O	1/10	$Ag_{0.05}Cu_{2.95}(BTC)_{1.97}$	0.09
Ag(0.17)/Cu-BTC/50%E	50% EtOH + 50% H_2O	1/6	$Ag_{0.05}Cu_{2.95}(BTC)_{1.97}$	0.09
Ag(1.00)/Cu-BTC/50%E	50% EtOH + 50% H_2O	1/1	$Ag_{0.06}Cu_{2.94}(BTC)_{1.96}$	0.11
Ag(1.50)/Cu-BTC/50%E	50% EtOH + 50% H_2O	3/2	$Ag_{0.06}Cu_{2.94}(BTC)_{1.96}$	0.11
Ag(0.10)/Cu-BTC/90%E	90% EtOH + 10% H_2O	1/10	$Ag_{0.07}Cu_{2.93}(BTC)_{1.95}$	0.12

[a]Solvent compositions based on volume fraction. [b]Based on EDS analysis.

species was obtained through fitting the XAES spectra of Cu LMM using XPSPEAK software.

Adsorption Measurement. The adsorption performance of parent and metal-modified Cu-BTC samples were evaluated by the adsorption capacities for three small organosulfur compounds (DMDS, ethyl sulfide, and 1-propanethiol). The model oils containing sulfides were prepared by dissolving DMDS, ethyl sulfide, or 1-propanethiol in *n*-hexane. A 0.2 g sample of solid sample was added into a 50 mL glass vessel containing 20 g of model oil. All adsorption experiments were carried out at 20 °C. The concentrations of sulfides in liquid phase were determined by using a GC-9560 gas chromatograph (Shanghai Huaai Chromatography Analysis Co., Ltd., Shanghai, China) equipped with a flame photometric detector and SE-30 capillary column (30 m × 0.32 mm × 1.0 μm).

The adsorption capacities for sulfides, Q (mg of S/g of adsorbent), can be calculated from the initial and equilibrated concentrations of DMDS, ethyl sulfide, or 1-propanethiol in liquid phase according to $Q = w(c_0 - c)/m \times 10^{-3}$, where w and m are the masses of the model oil and adsorbent (g), respectively; c_0 and c are the initial and equilibrated concentrations of sulfide in the model oil (mg of S/L).

RESULTS AND DISCUSSION

Sample Preparation and Characterization. A series of metal-modified Cu-BTC samples were prepared by employing different postsynthesis conditions provided in Table 1. The observed Ag/Cu ratios (the experimentally determined values) for postsynthesized samples were found to increase monotonically as the starting dosage of Ag^+ increased and almost reach a plateau at an experimentally used Ag/Cu of 0.1. When using a fixed starting Ag/Cu molar ratio for each postsynthesis experiment, the observed Ag/Cu ratios for different products show an increasing trend with increasing volume fractions of EtOH in the EtOH–H_2O solvent (0.02 for Ag(0.10)/Cu-BTC/W, 0.07 for Ag(0.10)/Cu-BTC/20%E, 0.09 for Ag(0.10)/Cu-BTC/50%E, and 0.12 for Ag(0.10)/Cu-BTC/90%E). It is indicated that ethanol enhances the impregnation of Ag species onto Cu-BTC largely. Because of the low solubility of $AgNO_3$ in ethanol, we could not achieve the successful loading of Ag on Cu-BTC by using only ethanol as the solvent. However, the exaggerating effect of ethanol on loading of Ag onto Ag(0.10)/Cu-BTC/90%E can be clearly realized by giving a higher observed Ag/Cu ratio (0.12) than those of Ag(0.17)/Cu-BTC/50%E (Ag/Cu ratio of 0.09) and Ag(1.00)/Cu-BTC/50%E (Ag/Cu ratio of 0.11).

Synthesized Cu-BTC has a well-defined pyramidal crystalline structure (see Figure S1a). After modification, the Ag(0.10)/Cu-BTC/90%E sample shows a rough surface (see Figure S1c), resulting from the Ag species. With the dosage of Ag^+ rising during the postsynthesis, there is an initially increasing loading and then the growing aggregation of Ag species on the crystal surface (see Figure S1e–h). In comparison with Ag(0.10)/Cu-BTC/50%E (see Figure S1f), the Ag(0.10)/Cu-BTC/90%E sample (see Figure S1c), which was postsynthesized in the solvent with a higher volume fraction of EtOH, shows better distribution of the Ag species on the surface, suggesting that EtOH can benefit the loading of Ag^+ onto Cu-BTC via not only enlarging the load amount but also improving the distribution. With the purpose of figuring out the distribution of Ag^+ in Cu-BTC, EDS surface scanning analysis was performed on Ag(0.10)/Cu-BTC/90%E (see Figure S2). It is indicated that Ag species are distributed uniformly on the crystal surface. It should be noticed that using a single solvent of water will result in remarkable destruction to Cu-BTC structure (see Figure S1d), which agrees with a previous report.[40] The surface area, pore volume, and pore size distribution of Cu-BTC samples before and after modification were measured and are shown in Table S2. It is indicated that the modification has no remarkable effect on the micropore structure of Cu-BTC, suggesting that metal modification (reduction of Cu(II) to Cu(I) as well as Ag loading) plays the main role in enhancing the sulfur adsorption ability of Cu-BTC.

To confirm their crystalline phases, powder XRD analyses were conducted on the parent and modified Cu-BTC samples (see Figure 1). All samples are observed to be a single phase of Cu-BTC.[41] The intensity of characteristic peaks stays consistent under a fixed solvent composition but varying load amounts of Ag. However, the intensity is diminished by a growing degree with increasing water content in the employed solvents. From Figure 1, Cu-BTC/E (using only EtOH as solvent, without Ag loading) and Ag(0.10)/Cu-BTC/90%E (using 90% EtOH + 10% H_2O as solvent, with Ag loading) show XRD patterns consistent with that of the parent Cu-BTC. Meanwhile, Ag(0.10)/Cu-BTC/W (using H_2O as solvent) exhibits the weakest diffraction intensity, supporting our conclusion from

DOI: 10.1021/acs.iecr.7b02392
Ind. Eng. Chem. Res. 2017, 56, 9541–9550

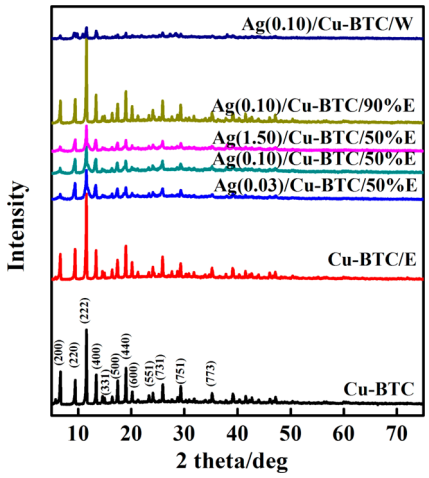

Figure 1. Powder X-ray diffraction patterns of Cu-BTC samples before and after modification.

SEM observations (see Figure S1d). Such an impact on the structure of Cu-BTC can be ascribed to the destructive effect resulting from H_2O. The binary EtOH−H_2O solvent with high EtOH content is considered to be a promising candidate in the postsynthesis process in order to prevent such a negative effect on the Cu-BTC framework.

Then we did Raman spectroscopic analyses in order to figure out the influences of the metal modification on the framework structure of Cu-BTC. In the spectrum of Cu-BTC (see Figure 2a), the wavenumber range of 1800−730 cm^{-1} is associated with the organic groups of the metal−organic structure. Specifically, the bands at 1610 and 1003 cm^{-1} are assigned to C═C vibration modes of the benzene ring.[42] The doublet at 1544 and 1460 cm^{-1} corresponds to the O−C−O asymmetrical and symmetrical stretching vibrations, respectively. The peaks at 826 and 740 cm^{-1} are ascribed to C−H out-of-plane bending vibrations of rings, while the peaks at 278, 449, and 502 cm^{-1} are associated with Cu(II)−O vibrations involving oxygen atoms of carboxylate bridges.[42,43] In addition, the peaks located at 170−195 cm^{-1} are assigned to the Cu−Cu stretching modes. Cu-BTC/E exhibits the quite consistent Raman spectrum to the parent Cu-BTC, suggesting that the solvent of ethanol preserves the framework structure very well. For three samples of Ag(0.10)/Cu-BTC/W, Ag(0.10)/Cu-BTC/50%E, and Ag(0.10)/Cu-BTC/90%E treated in H_2O-containing solvents, extremely similar structural changes can be detected from their Raman results. The peaks at 1400−1660 cm^{-1} are found to become broader and merge together. In the low-frequency region (ranging from 1000 to 170 cm^{-1}), all the peaks at 170, 278, 449, and 502 cm^{-1} disappear. All these spectral changes can be ascribed to the structure evolution of Cu-BTC during the postsynthesis modification, which are in accordance with the damped XRD intensity resulting from the increasing degree of chaos. Additionally, two new peaks at 219 and 930 cm^{-1}, which are responsible for the Cu(I)−$O_{0.5}$ vibrations,[44] appear in the spectrum curves of Ag(0.10)/Cu-BTC/50%E and Ag(0.10)/Cu-BTC/90%E, indicating the existence of Cu(I) in the modified Cu-BTC framework structures. We can speculate that reduction of Cu(II) to Cu(I) takes place in one of the two Cu(II) ions involved in the related paddle wheels during the modification (see Scheme 1), being partially responsible for the relevant structural evolution observed by XRD analysis. As compared to Ag(0.10)/Cu-BTC/50%E, Ag(0.10)/Cu-BTC/90%E has higher content of Cu(I) by

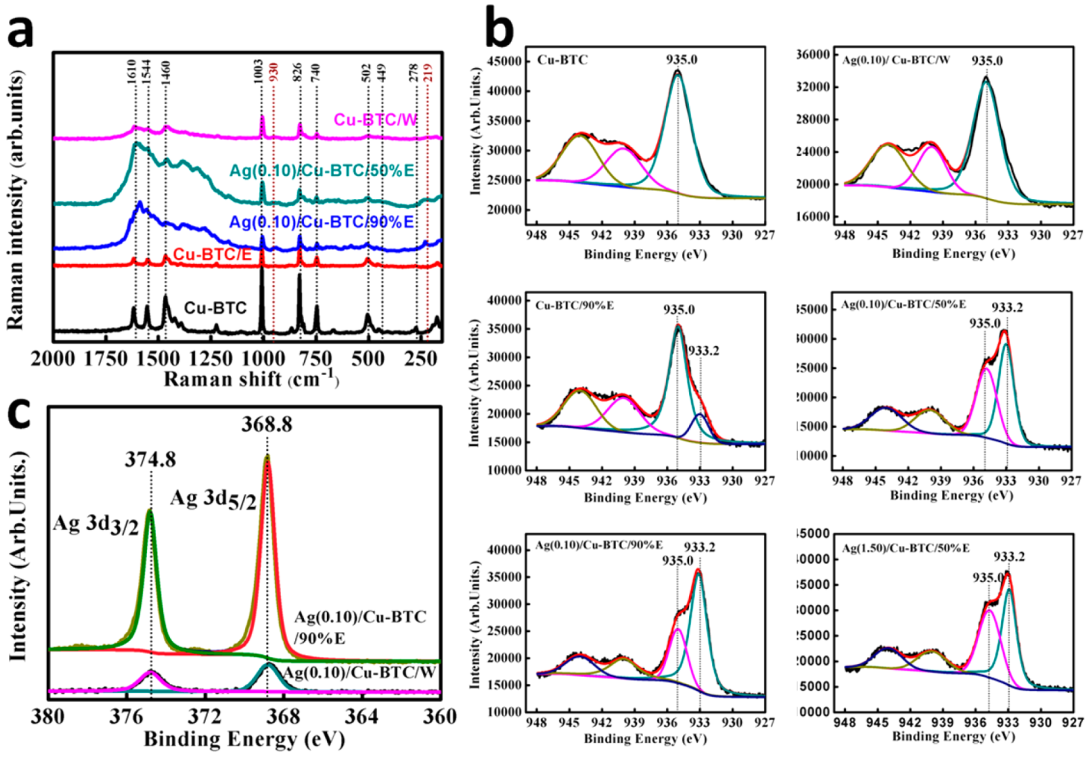

Figure 2. Characterization results for various Cu-BTC samples. (a) Raman spectra of Cu-BTC, Cu-BTC/E, Ag(0.10)/Cu-BTC/90%E, Ag(0.10)/Cu-BTC/50%E, and Cu-BTC/W. (b) Cu $2p_{3/2}$ XPS spectra of Cu-BTC, Cu-BTC/90%E, Ag(0.10)/Cu-BTC/90%E, Ag(0.10)/Cu-BTC/50%E, Ag(1.50)/Cu-BTC/50%E, and Ag(0.10)/Cu-BTC/W. (c) Ag 3d XPS spectra of Ag(0.10)/Cu-BTC/90%E and Ag(0.10)/Cu-BTC/W.

DOI: 10.1021/acs.iecr.7b02392
Ind. Eng. Chem. Res. 2017, 56, 9541−9550

Scheme 1. Reduction of Cu(II)-BTC to Cu(I)/Cu(II)-BTC and the Mechanism for Chemisorption of 1-Propanethiol on Modified Cu-BTC

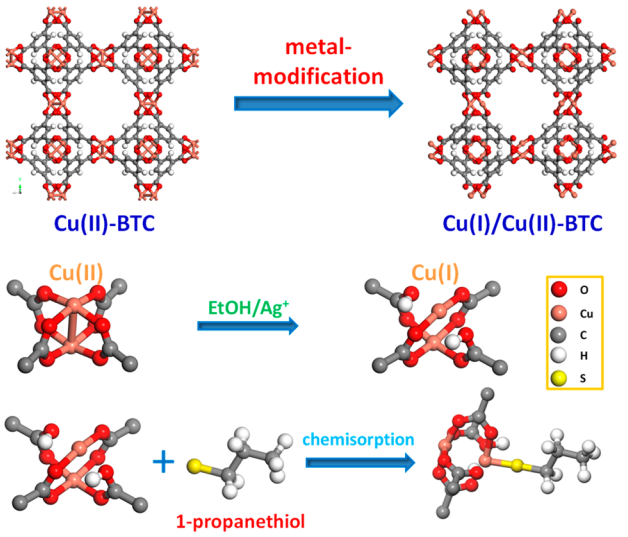

exhibiting the stronger spectral signals for the two corresponding peaks. It seems that the Ag−O stretching vibrations are barely detectable because of the extremely low content of Ag loaded on the samples.[45]

To further validate our speculation for the reduction of Cu(II) to Cu(I) in ethanol-containing solvents and obtain further insight into the metal modification on Cu-BTC via treatment in different solvents coupled with Ag loading, metal compositions of parent and modified Cu-BTC samples were revealed by XPS analyses (see Figure 2b,c). The binding energy was corrected by taking the C 1s peak at 284.5 eV as a reference. Like the parent Cu-BTC, Ag(0.10)/Cu-BTC/W displays the same binding energy at 935.0 eV, corresponding to Cu(II) $2p_{3/2}$.[46] Once EtOH was involved in the solvent, the modified Cu-BTC samples display an additional Cu(I) $2p_{3/2}$ peak (933.2 eV) as well as a weakened Cu(II) $2p_{3/2}$ signal relative to the parent Cu-BTC. To know the chemical state of Cu in different samples of Cu-BTC, Cu LMM XAES analyses were conducted on Cu-BTC, Ag(0.10)/Cu-BTC/50%E, and Ag(0.10)/Cu-BTC/90%E (see Figure S3). Only two overlapped Cu LMM Auger peaks arise at 572.6 and 570.0 eV, which correspond to Cu(I) and Cu(II), respectively. In view of the absence of the Cu LMM Auger peak at 567.9 eV (assigned to metallic Cu),[47,48] it can be concluded that the Cu(II) species are reduced into Cu(I) ones successfully during the modification. Also, the binding energies are confirmed consistent with the values observed from Cu(I) and Cu(II) complexes but 0.5−1.5 eV higher than those of their corresponding oxides.[49−52] Furthermore, the Cu(I)/Cu(II) molar ratios for different samples were derived from the integration of XPS peaks (see Table S1). All Cu species for the parent Cu-BTC and Ag(0.10)/Cu-BTC/W were confirmed to be Cu(II). From the results of XPS as well as Raman characterizations, thanks to the mutable skeleton structure of the Cu-BTC,[53] the reduction of Cu(II) to Cu(I) in the Cu-BTC framework can take place during the modification process, in which the ethanol acts as not only a solvent but also a reducing agent. One reasonable explanation is that the ethanol molecules in solution are first chemisorbed and then spilt over on the surface of Cu-BTC (see Scheme 1). Hereafter, the spilt-over species reach the coordinated Cu(II)−O's and interacts with them, leading to the formation of lower-valence Cu(I). With the reduction of Cu(II) to Cu(I), the carboxylate bridge is detached from the paddle wheel of the Cu-BTC structure.[40] By varying the compositions of binary EtOH−H_2O solvents, the modified Cu-BTC samples display quantitatively changed Cu(I)/Cu(II) molar ratios. Specifically, Ag(0.10)/Cu-BTC/90%E gives a larger Cu(I)/Cu(II) ratio (1.89) as compared to Ag(0.10)/Cu-BTC/50%E (1.18).

Moreover, it is interesting that the introduction of Ag dramatically contributes to the remarkable enhancement on reduction of Cu(II). Ag^+ ions act as the catalyst during the oxidation−reduction reaction converting Cu(II) to Cu(I). We find this is very similar to the classical reaction of catalytic oxidation of ethanol. Ag-loaded samples show a much higher Cu(I)/Cu(II) ratio than Cu-BTC/90%E (Cu(I)/Cu(II) of 0.36) without Ag impregnation. Once the content of ethanol in solvent is fixed, the Cu(I)/Cu(II) ratio can finally reach a plateau with Ag/Cu ratios increasing. By integrating the XPS peaks associated with Ag $3d_{3/2}$ and Ag $3d_{5/2}$ located, respectively, at 374.8 and 368.8 eV (see Figure 2c), we can find that Ag(0.10)/Cu-BTC/90%E has better Ag loading than Ag(0.10)/Cu-BTC/W, which is accordance with our previous results of composition measurement as well as SEM analysis. In addition, our results from ICP-AES analyses on contents of metal cations left in the used solvents also support the current conclusion by showing the 35 times higher concentration of

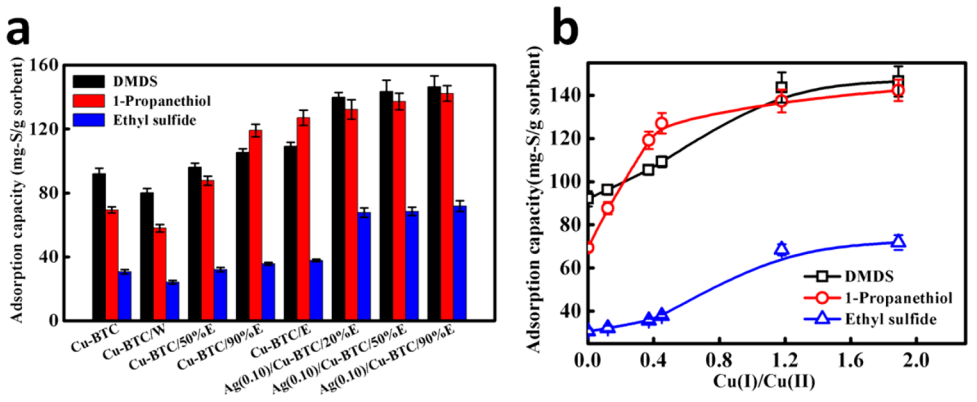

Figure 3. (a) Adsorption capacities of Cu-BTC samples before and after modification. (b) Relationship between adsorption capacities for sulfides and Cu(I)/Cu(II) molar ratios of Cu-BTC.

DOI: 10.1021/acs.iecr.7b02392
Ind. Eng. Chem. Res. 2017, 56, 9541−9550

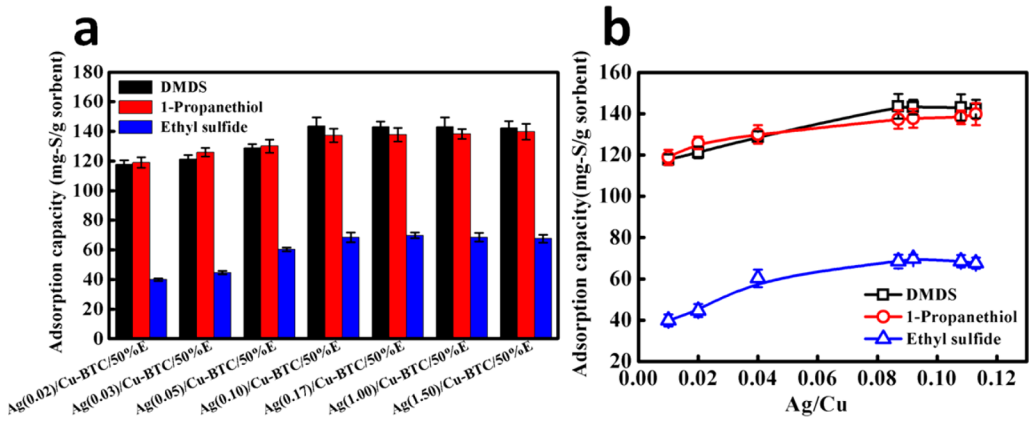

Figure 4. (a) Adsorption capacities of modified Cu-BTC samples with different molar ratios of Ag/Cu. (b) Relationship between adsorption capacities for sulfides and Ag/Cu molar ratios of Cu-BTC.

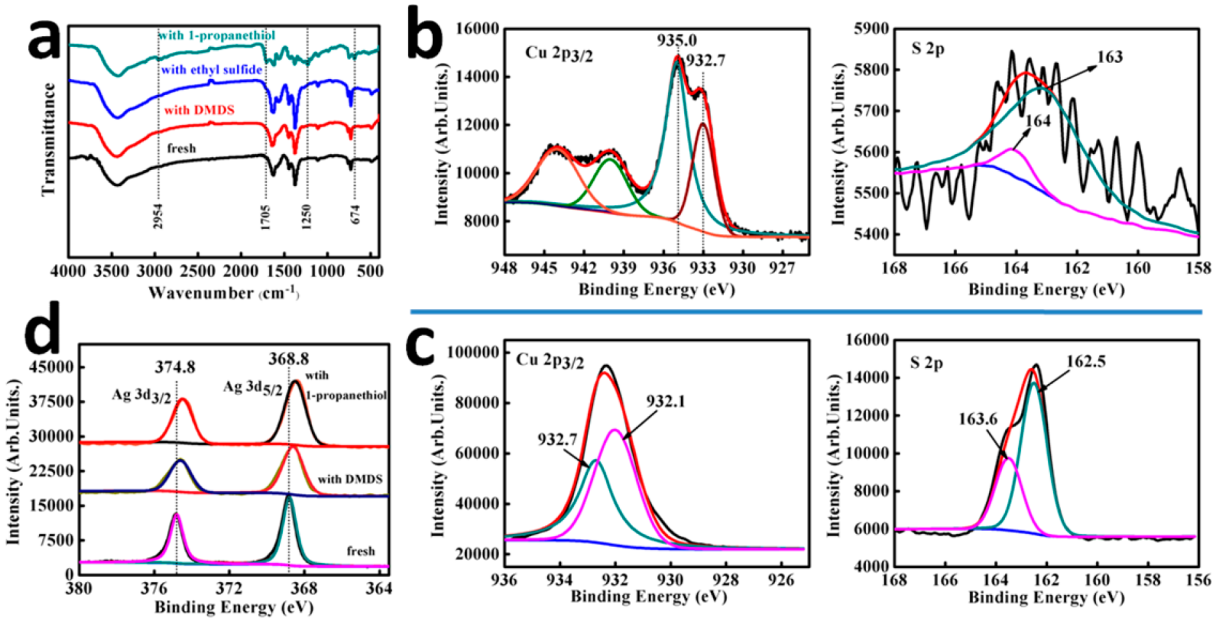

Figure 5. (a) FTIR spectra of fresh Ag(0.10)/Cu-BTC/50%E and samples after adsorbing DMDS, ethyl sulfide, and 1-propanethiol. (b) XPS spectra of Ag(0.10)/Cu-BTC/50%E after adsorbing DMDS. (c) XPS spectra of Ag(0.10)/Cu-BTC/50%E after adsorbing 1-propanethiol. (d) Ag 3d XPS spectra of fresh Ag(0.10)/Cu-BTC/50%E and samples with DMDS (138.23 mg of S/g of sorbent) and 1-propanethiol (135.76 mg of S/g of sorbent).

Ag^+ in water than that in 90% EtOH + 10% H_2O solvent (596.03 mg/L vs 16.97 mg/L). Besides, we can conclude that most of the Ag species are introduced to the Cu-BTC through loading on the surface rather than exchanging with Cu^{2+} according to our ICP-AES analyses. All of present results clearly indicate that ethanol can improve the loading of Ag onto Cu-BTC. On the other hand, Ag is found to be able to catalyze the reduction of Cu(II) to Cu(I) in the Cu-BTC structure when employing ethanol as reducing agent. It seems that the combination of ethanol involvement and Ag loading results in a synergistic effect on the metal modification of Cu-BTC. As a result, the reduction of Cu(II) to Cu(I) in Cu-BTC can be well manipulated via controlling the composition of binary EtOH−H_2O solvent and the Ag loading in order to achieve the well-defined Cu(I)/Cu(II)-BTC which can be expected to have remarkable adsorption of small organosulfur compounds.[38,54]

Effect of Tuned Reduction of Cu(II) to Cu(I) on Adsorption Activity. To determine the quantitative influence of metal modification on adsorption of organosulfurs on Cu-BTC, a series of batch experiments of organosulfur uptakes from model oils were conducted using various metal-modified Cu-BTC samples at room temperature (see Figures 3 and 4). The model oils have the initial concentrations of DMDS of 2500 mg of S/L, 1-propanethiol of 2200 mg of S/L, and ethyl sulfide of 1100 mg of S/L, respectively. The relationships of adsorption capacity versus Cu(I)/Cu(II) molar ratio and adsorption capacity versus Ag/Cu molar ratio are displayed in Figures 3 and 4, respectively. From Figure 3a, the adsorption capacities for organosulfur compounds were significantly improved after undergoing ethanol treatment. Nevertheless, the sample treated in water, Cu-BTC/W, gives reduced adsorption capacities, resulting from the structural deconstruction made by water. The increasing contents of ethanol in the EtOH−H_2O solvents are found beneficial to the enhancement of adsorption capacity. With the Cu(I)/Cu(II) ratio increasing, the adsorption capacities for all three organosulfurs initially rapidly rise and reach the different plateaus at almost the same Cu(I)/Cu(II) of 1.2 (see Figure 3b). Employing metal

DOI: 10.1021/acs.iecr.7b02392
Ind. Eng. Chem. Res. 2017, 56, 9541−9550

modification on Cu-BTC, the adsorption capacities for DMDS, ethyl sulfide, and 1-propanethiol can be largely increased by around 59% (from 92.07 mg of S/g for the parent Cu-BTC to 146.39 mg of S/g for Ag(0.10)/Cu-BTC/90%E), 134% (from 30.69 to 71.83 mg of S/g), and 105% (from 69.38 to 142.29 mg of S/g), respectively. From previous investigations, we learned that DMDS adsorption capacity in several kinds of modified zeolite are in the range 2.5−82.4 mg of S/g.[55,56] A recent work mentioned the saturated adsorption capacity of 157.4 mg of S/g for modified Y zeolites,[57] while the metal-modified Cu-BTC has the adsorption capacity of 200−250 mg of S/g (see Figure S5). For the parent Cu-BTC, the adsorption capacity of ethanethiol has been reported to be 65.3 mg of S/g,[58] while the adsorption capacity of 1-propanethiol is determined to be 69.38 mg of S/g in this work. Furthermore, the modified Cu-BTC samples are found to display 1.7−2 times higher adsorption capacities than the parent Cu-BTC. Consequently, the increase of adsorption capacity of 1-propanethiol shows a larger slope as compared to that of DMDS or ethyl sulfide. Herein, we present the quantitative relationship between Cu(I) contents in Cu-BTC and their adsorption capacities of small organosulfur compounds. Additionally, as the composition of the binary EtOH−H_2O solvent is fixed, the sulfide adsorption capacities of modified Cu-BTC samples show a rapid rise with increasing Ag/Cu ratios and finally reach the different plateaus at the same Ag/Cu ratio of around 0.087 (see Figure 4b). Our previous results have indicated the promising catalysis effect of loaded Ag onto Cu-BTC on the reduction of Cu(II) to Cu(I). The increase of Ag loading benefits the reduction reaction, resulting in an increasing Cu(I)/Cu(II) and, therefore, a reasonable varying trend of adsorption capacities (like the trend in Figure 3b). It should be noted that the adsorption capacity will remain a constant once the content of Ag rises to a fixed value. More Ag loading is barely helpful to the improvement of adsorption capacity. Current results lead us to conclude that the loaded Ag species enhance the adsorption capacity via playing the role of catalyst rather than directly available adsorption sites for organosulfur molecules.

Mechanism of Adsorption. To reveal the underlying mechanism for the adsorption of DMDS, ethyl sulfide, and 1-propanethiol on metal-modified Cu-BTC, combined techniques including FTIR and XPS analyses were employed to characterize the fresh and sulfide-saturated samples of Ag(0.10)/Cu-BTC/50%E. The samples saturated with DMDS and ethyl sulfide have FTIR spectra extremely similar to that of the fresh adsorbent sample (see Figure 5a). The band at 1617.7 cm^{-1} is assigned to the symmetric stretching vibration of the carboxylate group, while the bands at 1442.3 and 1372.9 cm^{-1} correspond to the asymmetric mode.[59] The appearance of the band at 3424.5 cm^{-1} can be attributed to the incomplete dehydration of samples.[60] By comparison, 1-propanethiol-saturated sample shows additional characteristic absorption peaks, with the bands situated at 1706.6 and 1249.6 cm^{-1} corresponding to the carboxylate protonation vibration as well as the band at 673.9 cm^{-1} assigned to Cu−S vibration.[61,62] An additional peak appearing at 2953.6 cm^{-1} in the spectrum is attributed to the propyl group of adsorbed 1-propanethiol.[63] These results indicate that chemical adsorption occurs most likely on the Cu sites of the MOF structure.

Furthermore, XPS analyses on the fresh and spent Ag(0.10)/Cu-BTC/50%E samples were performed in order to determine the chemical state of constituent elements and further confirm the underlying adsorption mechanism. For the Cu $2p_{3/2}$ spectrum of the sample exhausted from DMDS adsorption (see Figure 5b), 0.5 eV lower binding energies for Cu(I) $2p_{3/2}$ (moving from 933.2 to 932.7 eV) and Cu(II) $2p_{3/2}$ (moving from 935.0 to 934.5 eV) can be observed as compared with the fresh sample of Ag(0.10)/Cu-BTC/50%E. The shifts in binding energy indicate the direct interaction involved among Cu(I), Cu(II), and sulfide molecules. Meanwhile, the peak located at 164.0 eV in the S $2p_{1/2}$ spectrum can be attributed to DMDS.[64] The Cu $2p_{3/2}$ and S $2p_{1/2}$ spectra of ethyl sulfide saturated Ag(0.10)/Cu-BTC/50%E are confirmed similar to that of the sample hosting DMDS. After adsorbing 1-propanethiol (see Figure 5c), the asymmetrical Cu $2p_{3/2}$ XPS peak could be resolved into two peaks centered at 932.1 and 932.7 eV. The peak situated at 934.5 eV is replaced with a new one at 932.1 eV, which is ascribed to the combined group of O−Cu−S−C_3H_7. The S $2p_{1/2}$ peak could be decomposed into two peaks located at 162.5 and 163.6 eV, which are assigned to −Cu−S− and physisorbed bulk C_3H_7SH, respectively.[31,65] We can also be informed that there are no bonds directly formed between Ag species and S atoms from the Ag 3d spectrum of the Ag(0.10)/Cu-BTC/50%E sample after adsorbing DMDS (see Figure 5d). The Ag species act as a catalyst for the reduction of Cu(II) into Cu(I) that we have aforementioned.

These XPS findings are in accordance with previous spectral analysis results. 1-Propanethiol exhibits a different adsorption mechanism from DMDS and ethyl sulfide because of their distinct steric effect for the accessibility to the metal adsorption sites. Cu-BTC has open sites of copper that exhibit Lewis acidity and, thus, is able to interact with the metal site accessed sulfur compounds having lone electron pairs, such as 1-propanethiol. Owing to the small hydrogen atom bound to sulfur at the one end, 1-propanethiol is accessible to the open Cu sites via coordination. However, it is difficult for DMDS and ethyl sulfide to reach the open metal sites because of their strong steric hindrance.[37] The weak guest−host interactions between Cu-BTC structures and these two sulfide compounds, therefore, can be observed. Such weak interactions most likely originate from the electrostatic force surrounding copper as well as the intermolecular coordination, which is supported by the XPS results and the color evolution (see Figure S4) of the samples during adsorption of these sulfides. There is a remarkable color difference between Ag(0.10)/Cu-BTC/50%E samples before and after adsorbing 1-propanethiol (from cyan to olive). In contrast, little variation of evolution for the adsorbent can be observed during the course of adsorbing DMDS or ethyl sulfide. The strong affinity between Cu and S may result in the breakage of the Cu−O bond, which was originally modifiable, and the release of carboxylic groups (see Scheme 1). These reactions create a different chemical environment for Cu and eventually result in the color change from cyan to olive.

Batch Adsorption Measurements. Batch liquid phase adsorption experiments for DMDS, 1-propanethiol, and ethyl sulfide on Ag(0.10)/Cu-BTC/50%E were carried out at 278, 293, and 308 K. The adsorption isotherms were described by employing model oils containing different starting concentrations of organosulfurs (ranging from 500 to 7000 mg of S/L) (see Figures S5−S7). By using the Freundlich model, given as eq 1, all adsorption isotherms can be explained well. The fitted curves are plotted as solid lines in Figures S5−S7. Their thermodynamic parameters are also extracted and listed in Table S3.

DOI: 10.1021/acs.iecr.7b02392
Ind. Eng. Chem. Res. 2017, 56, 9541−9550

$$q_e = K_f C_e^{1/n} \quad (1)$$

where q_e is the sulfide uptake at equilibrium state (mg of S/g of sorbent), C_e is the concentration of the organosulfurs at equilibrium state (mg of S/L), K_f is the Freundlich equilibrium constant, and n is the constant parameter.

Both DMDS and ethyl sulfide have decreasing equilibrium adsorption amounts with adsorption temperature increasing (see Figures S5 and S6), which can be observed in a general physical adsorption process. As for DMDS and ethyl sulfide, the exothermic enthalpies of adsorption, ΔH, are 8.85 and 13.41 kJ/mol (see Table S3), respectively. An interesting fact is that the q_e of 1-propanethiol rises with an increasing adsorption temperature (see Figure S7), suggesting the endothermic chemical interactions involved in the adsorption of 1-propanethiol onto Ag(0.10)/Cu-BTC/50%E. The endothermic heat of adsorption is evaluated to be 14.97 kJ/mol. Such a heat effect can result from a combination of endothermic chemisorption and exothermic physisorption. Similar chemisorption results have been found in our previous study on the adsorption of DMDS on ion-exchanged ZSM-5 zeolite.[66]

CONCLUSIONS

In summary, we have demonstrated a strategy for metal modification of Cu-BTC via the well-controlled reduction of Cu(II) to Cu(I) in Cu-BTC using ethanol as the reducing agent coupled with loaded Ag as catalyst under mild conditions. Combined characterization results from FTIR, Raman, XPS, XAES, SEM, and EDS analyses confirmed the successful modification and examined their structural changes. Increase in either EtOH content in EtOH−H_2O solvent or Ag loading can promote the reduction of Cu(II) to Cu(I). In addition, ethanol contributes to the loading of Ag onto Cu-BTC via enlarging loading amount as well as improving distribution. As a result, the modified Cu-BTC samples exhibit largely enhanced adsorption capacities for organosulfurs (DMDS, ethyl sulfide, and 1-propanethiol). Such a performance enhancement along with structural evolution provides important implications for the tunable modification of metal−organic framework structures and benefits to the function of their molecular architectures.

ASSOCIATED CONTENT

Supporting Information

The Supporting Information is available free of charge on the ACS Publications website at DOI: 10.1021/acs.iecr.7b02392.

N_2 adsorption, SEM images, EDS surface scanning analyses, Cu LMM XAES spectra, sample pictures, adsorption isotherms, and tables (PDF)

AUTHOR INFORMATION

Corresponding Author

*E-mail: sunhui@ecust.edu.cn.

ORCID

Hui Sun: 0000-0002-8544-756X

Jichang Liu: 0000-0002-5295-1778

Di Wu: 0000-0001-6879-321X

Notes

The authors declare no competing financial interest.

ACKNOWLEDGMENTS

This work is financially supported by the Training Program of the Major Research Plan of the National Natural Science Foundation of China (Grant 91634112), the Natural Science Foundation of Shanghai (Grant 16ZR1408100), the Fundamental Research Funds for the Central Universities of China (Grant 22A201514010) and the Open Project of State Key Laboratory of Chemical Engineering (SKL-ChE-16C01). D.W. acknowledges institutional funds from the Gene and Linda Voiland School of Chemical Engineering and Bioengineering at Washington State University.

ABBREVIATIONS

LPG = liquefied petroleum gas
NG = natural gas
ADS = adsorption desulfurization
HDS = hydrodesulfurization
SEM = scanning electron microscopy
EDS = energy-dispersive spectrometry
XRD = X-ray diffraction
FTIR = Fourier transform infrared spectroscopy
XPS = X-ray photoelectron spectroscopy
DMDS = dimethyl disulfide
ICP-AES = inductively coupled plasma atomic emission spectrometer

REFERENCES

(1) Hou, X.; Marin-Flores, O.; Kwon, B. W.; Kim, J.; Norton, M. G.; Ha, S. Gasoline-fueled solid oxide fuel cell using MoO_2-Based Anode. *J. Power Sources* **2014**, *268*, 546.

(2) Rezaei, F.; Rownaghi, A. A.; Monjezi, S.; Lively, R. P.; Jones, C. W. SO_x/NO_x Removal from Flue Gas Streams by Solid Adsorbents: A Review of Current Challenges and Future Directions. *Energy Fuels* **2015**, *29*, 5467.

(3) Sun, W.; Lin, L. C.; Peng, X.; Smit, B. Computational screening of porous metal - organic frameworks and zeolites for the removal of SO_2 and NO_x from flue gases. *AIChE J.* **2014**, *60*, 2314.

(4) Wang, L.; Yang, R. T.; Sun, C. L. Graphene and other carbon sorbents for selective adsorption of thiophene from liquid fuel. *AIChE J.* **2013**, *59*, 29.

(5) Hernández-Maldonado, A. J.; Yang, R. T. Desulfurization of Commercial Liquid Fuels by Selective Adsorption via π-Complexation with Cu(I)−Y Zeolite. *Ind. Eng. Chem. Res.* **2003**, *42*, 3103.

(6) Pandey, R. A.; Biswas, R.; Chakrabarti, T.; Devotta, S. Flue Gas Desulfurization: Physicochemical and Biotechnological Approaches. *Crit. Rev. Environ. Sci. Technol.* **2005**, *35* (6), 571.

(7) Shiraishi, Y.; Tachibana, K.; Hirai, T.; Komasawa, I. Desulfurization and Denitrogenation Process for Light Oils Based on Chemical Oxidation followed by Liquid−Liquid Extraction. *Ind. Eng. Chem. Res.* **2002**, *41*, 4362.

(8) Huang, C. P.; Chen, B. H.; Zhang, J.; Liu, Z. C.; Li, Y. X. Desulfurization of Gasoline by Extraction with New Ionic Liquids. *Energy Fuels* **2004**, *18*, 1862.

(9) Yang, R. T.; Hernández-Maldonado, A. J.; Yang, F. H. Desulfurization of transportation fuels with zeolites under ambient conditions. *Science* **2003**, *301*, 79.

(10) Ma, X.; Velu, S.; Kim, J. H.; Song, C. Deep desulfurization of gasoline by selective adsorption over solid adsorbents and impact of analytical methods on ppm-level sulfur quantification for fuel cell applications. *Appl. Catal., B* **2005**, *56*, 137.

(11) Deliyanni, E.; Seredych, M.; Bandosz, T. J. Interactions of 4,6-dimethyldibenzothiophene with the surface of activated carbons. *Langmuir* **2009**, *25*, 9302.

(12) Li, F. T.; Wu, B.; Liu, R. H.; Wang, X. J.; Chen, L. J.; Zhao, D. S. An inexpensive N-methyl-2-pyrrolidone-based ionic liquid as efficient

DOI: 10.1021/acs.iecr.7b02392
Ind. Eng. Chem. Res. 2017, 56, 9541−9550

extractant and catalyst for desulfurization of dibenzothiophene. *Chem. Eng. J.* **2015**, *274*, 192.
(13) Cammarano, C.; Huguet, E.; Cadours, R.; Leroi, C.; Coq, B.; Hulea, V. Selective transformation of methyl and ethyl mercaptans mixture to hydrocarbons and H_2S on solid acid catalysts. *Appl. Catal., B* **2014**, *156*−*157*, 128.
(14) Yi, D.; Huang, H.; Meng, X.; Shi, L. Adsorption−desorption behavior and mechanism of dimethyl disulfide in liquid hydrocarbon streams on modified Y zeolites. *Appl. Catal., B* **2014**, *148*−*149*, 377.
(15) Seredych, M.; Lison, J.; Jans, U.; Bandosz, T. J. Textural and chemical factors affecting adsorption capacity of activated carbon in highly efficient desulfurization of diesel fuel. *Carbon* **2009**, *47*, 2491.
(16) Hernández-Maldonado, A. J.; Yang, R. T. New Sorbents for Desulfurization of Diesel Fuels via π Complexation: Layered Beds and Regeneratio. *AIChE J.* **2004**, *50*, 791.
(17) Farzin Nejad, N. F.; Shams, E.; Amini, M. K.; Bennett, J. C. Ordered mesoporous carbon CMK-5 as a potential sorbent for fuel desulfurization: Application to the removal of dibenzothiophene and comparison with CMK-3. *Microporous Mesoporous Mater.* **2013**, *168*, 239.
(18) Li, W. L.; Tang, H.; Zhang, T.; Li, Q.; Xing, J. M.; Liu, H. Z. Ultra-deep desulfurization adsorbents for hydrotreated diesel with magnetic mesoporous aluminosilicates. *AIChE J.* **2010**, *56*, 1391.
(19) Srivastav, A.; Srivastava, V. C. Adsorptive desulfurization by activated alumina. *J. Hazard. Mater.* **2009**, *170*, 1133.
(20) Xiao, J.; Sitamraju, S.; Chen, Y.; Janik, M.; Song, J. Air-Promoted Adsorptive Desulfurization over $Ti_{0.9}Ce_{0.1}O_2$ Mixed Oxides from Diesel Fuel under Ambient Conditions. *ChemCatChem* **2013**, *5*, 3582.
(21) Liu, J.; Wang, Y.; Benin, A. I.; Jakubczak, P.; Willis, R. R.; LeVan, M. D. CO_2/H_2O adsorption equilibrium and rates on metal-organic frameworks: HKUST-1 and Ni/DOBDC. *Langmuir* **2010**, *26*, 14301.
(22) Furukawa, H.; Cordova, K. E.; O'Keeffe, M.; Yaghi, O. M. The Chemistry and Applications of Metal-Organic Frameworks. *Science* **2013**, *341*, 1230444.
(23) Li, J. R.; Sculley, J.; Zhou, H. C. Metal-organic frameworks for separations. *Chem. Rev.* **2012**, *112*, 869.
(24) Murray, L. J.; Dincă, M.; Long, J. R. Hydrogen storage in metal-organic frameworks. *Chem. Soc. Rev.* **2009**, *38*, 1294.
(25) Stock, N.; Biswas, S. Synthesis of metal-organic frameworks (MOFs): routes to various MOF topologies, morphologies, and composites. *Chem. Rev.* **2012**, *112*, 933.
(26) Kuppler, R. J.; Timmons, D. J.; Fang, Q. R.; Li, J.-R.; Makal, T. A.; Young, M. D.; Yuan, D.; Zhao, D.; Zhuang, W.; Zhou, H.-C. Potential applications of metal-organic frameworks. *Coord. Chem. Rev.* **2009**, *253*, 3042.
(27) Mueller, U.; Schubert, M.; Teich, F.; Puetter, H.; Schierle-Arndt, K.; Pastre, J. Metal-organic frameworks - prospective industrial applications. *J. Mater. Chem.* **2006**, *16*, 626.
(28) Cychosz, K. A.; Wongfoy, A. G.; Matzger, A. J. Liquid phase adsorption by microporous coordination polymers: removal of organosulfur compounds. *J. Am. Chem. Soc.* **2008**, *130*, 6938.
(29) Hong, D. Y.; Hwang, Y. K.; Serre, C.; Férey, G.; Chang, J. S. Porous Chromium Terephthalate MIL - 101 with Coordinatively Unsaturated Sites: Surface Functionalization, Encapsulation, Sorption and Catalysis. *Adv. Funct. Mater.* **2009**, *19*, 1537.
(30) Yoon, J. W.; Seo, Y. K.; Hwang, Y. K.; Chang, J. S.; Leclerc, H.; Wuttke, S.; Bazin, P.; Vimont, A.; Daturi, M.; Bloch, E.; et al. Controlled reducibility of a metal-organic framework with coordinatively unsaturated sites for preferential gas sorption. *Angew. Chem., Int. Ed.* **2010**, *49*, 5949.
(31) Li, Y.; Wang, L. J.; Fan, H. L.; Shangguan, J.; Wang, H.; Mi, J. Removal of Sulfur Compounds by a Copper-Based Metal Organic Framework under Ambient Conditions. *Energy Fuels* **2015**, *29*, 298.
(32) Wu, L. M.; Xiao, J.; Wu, Y.; Xian, S. K.; Miao, G.; Wang, H. H.; Li, Z. A combined experimental/computational study on the adsorption of organosulfur compounds over metal-organic frameworks from fuels. *Langmuir* **2014**, *30*, 1080.
(33) Ahmed, I.; Jhung, S. H. Adsorptive desulfurization and denitrogenation using metal-organic frameworks. *J. Hazard. Mater.* **2016**, *301*, 259.
(34) Song, X. L.; Sun, L. B.; He, G. S.; Liu, X. Q. Isolated Cu(I) sites supported on β-cyclodextrin: an efficient π-complexation adsorbent for thiophene capture. *Chem. Commun.* **2011**, *47*, 650.
(35) Neubauer, R.; Weinlaender, C.; Kienzl, N.; Schroettner, H.; Hochenauer, C. Adsorptive Desulfurization: Fast On-Board Regeneration and the Influence of Fatty Acid Methyl Ester on Desulfurization and in Situ Regeneration Performance of a Silver-Based Adsorbent. *Energy Fuels* **2016**, *30*, 5174.
(36) Khan, N. A.; Jhung, S. H. Adsorptive removal of benzothiophene using porous copper-benzenetricarboxylate loaded with phosphotungstic acid. *Fuel Process. Technol.* **2012**, *100*, 49.
(37) Szanyi, J.; Daturi, M.; Clet, G.; Baer, D. R.; Peden, C. H. F. Well-studied Cu-BTC still serves surprises: evidence for facile Cu^{2+}/Cu^{+} interchange. *Phys. Chem. Chem. Phys.* **2012**, *14*, 4383.
(38) Qin, J. X.; Tan, P.; Jiang, Y.; Liu, X.-Q.; He, Q.-X.; Sun, L.-B. Functionalization of metal-organic frameworks with cuprous sites using vapor-induced selective reduction: efficient adsorbents for deep desulfurization. *Green Chem.* **2016**, *18*, 3210.
(39) Ahmed, A.; Robertson, C. M.; Steiner, A.; Whittles, T.; Ho, A.; Dhanak, V.; Zhang, H. F. Cu(I)Cu(II)BTC, a microporous mixed-valence MOF via reduction of HKUST-1. *RSC Adv.* **2016**, *6*, 8902.
(40) Todaro, M.; Buscarino, G.; Sciortino, L.; Alessi, A.; Messina, F.; Taddei, M.; Ranocchiari, M.; Cannas, M.; Gelardi, F. M. Decomposition Process of Carboxylate MOF HKUST-1 Unveiled at the Atomic Scale Level. *J. Phys. Chem. C* **2016**, *120*, 12879.
(41) Nguyen, L. T. L.; Nguyen, T. T.; Nguyen, K. D.; Phan, N. T. S. Metal-organic framework MOF-199 as an efficient heterogeneous catalyst for the aza-Michael reaction. *Appl. Catal., A* **2012**, *425*−*426*, 44.
(42) Prestipino, C.; Regli, L.; Vitillo, J. G.; Bonino, F.; Damin, A.; Lamberti, C.; Zecchina, A.; Solari, P. L.; Kongshaug, K. O.; Bordiga, S. Local Structure of Framework Cu(II) in HKUST-1 Metallorganic Framework: Spectroscopic Characterization upon Activation and Interaction with Adsorbates. *Chem. Mater.* **2006**, *18*, 1337.
(43) Dhumal, N. R.; Singh, M. P.; Anderson, J. A.; Kiefer, J.; Kim, H. J. Molecular Interactions of a Cu-Based Metal-Organic Framework with a Confined Imidazolium-Based Ionic Liquid: A Combined Density Functional Theory and Experimental Vibrational Spectroscopy Study. *J. Phys. Chem. C* **2016**, *120*, 3295.
(44) Sahai, A.; Goswami, N.; Kaushik, S. D.; Tripathi, S. $Cu/Cu_2O/CuO$ Nanoparticles: Novel Synthesis by Exploding Wire Technique and Extensive Characterization. *Appl. Surf. Sci.* **2016**, *390*, 974.
(45) Li, C.; Yang, C.; Xu, S. C.; Zhang, C.; Li, Z.; Liu, X. Y.; Jiang, S. Z.; Huo, Y.; Liu, A.; Man, B. Ag_2O@Ag core-shell structure on PMMA as low-cost and ultra-sensitive flexible surface-enhanced Raman scattering substrate. *J. Alloys Compd.* **2017**, *695*, 1677.
(46) Le, X. T.; Viel, P.; Sorin, A.; Palacin, S.; Jegou, P. Electrochemical behaviour of polyacrylic acid coated gold electrodes: An application to remove heavy metal ions from wastewater. *Electrochim. Acta* **2009**, *54*, 6089.
(47) Fei, H.; Cohen, S. M. Metalation of a thiocatechol-functionalized Zr(IV)-based metal-organic framework for selective C-H functionalization. *J. Am. Chem. Soc.* **2015**, *137*, 2191.
(48) Bae, Y. S.; Farha, O. K.; Spokoyny, A. M.; Mirkin, C. A.; Hupp, J. T.; Snurr, R. Q. Carborane-based metal-organic frameworks as highly selective sorbents for CO_2 over methane. *Chem. Commun.* **2008**, *35*, 4135.
(49) Tahir, D.; Tougaard, S. Electronic and optical properties of Cu, CuO and Cu_2O studied by electron spectroscopy. *J. Phys.: Condens. Matter* **2012**, *24*, 175002.
(50) Ghijsen, J.; Tjeng, L. H.; van Elp, J.; Eskes, H.; Westerink, J.; Sawatzky, G. A.; Czyzyk, M. T. Electronic structure of Cu_2O and CuO. *Phys. Rev. B: Condens. Matter Mater. Phys.* **1988**, *38*, 11322.
(51) Sun, Y. H.; Yu, J. H.; Jin, X. J.; Song, J. F.; Xu, J. Q.; Ye, L. Synthesis and characterization of first hetero-nuclear molybdenum

DOI: 10.1021/acs.iecr.7b02392
Ind. Eng. Chem. Res. 2017, 56, 9541−9550

copper cluster with highly delocalized Cu(I)/Cu(II). *Inorg. Chem. Commun.* **2006**, *9*, 1087.
(52) Gagne, R. R.; Allison, J. L.; Koval, C. A.; Mialki, W. S.; Smith, T. J.; Walton, R. A. The x-ray photoelectron spectra of inorganic molecules. 25. X-ray photoelectron spectra of copper(I) and copper(II) complexes derived from macrocyclic ligands. *J. Am. Chem. Soc.* **1980**, *102*, 1905.
(53) Psofogiannakis, G. M.; Froudakis, G. E. Theoretical Explanation of Hydrogen Spillover in Metal-Organic Frameworks. *J. Phys. Chem. C* **2011**, *115*, 4047.
(54) Zhang, Q.; Shi, L.; Meng, X. Deep adsorption desulfurization of liquid petroleum gas by copper-modified bentonite. *RSC Adv.* **2016**, *6*, 9589.
(55) Zhao, Y.; Shen, B.; Sun, H. Adsorptive removal of dimethyl disulfide from methyl tert-butyl ether using an Ag-exchanged ZSM-5 zeolite. *RSC Adv.* **2016**, *6*, 93086.
(56) Lee, J.; Beum, H. T.; Ko, C. H.; Park, S. Y.; Park, J. H.; Kim, J.-N.; Chun, B.-H.; Kim, S. H. Adsorptive Removal of Dimethyl Disulfide in Olefin Rich C4 with Ion-Exchanged Zeolites. *Ind. Eng. Chem. Res.* **2011**, *50*, 6382.
(57) Yi, D.; Huang, H.; Meng, X.; Shi, L. Adsorption−desorption behavior and mechanism of dimethyl disulfide in liquid hydrocarbon streams on modified Y zeolites. *Appl. Catal., B* **2014**, *148−149*, 377.
(58) Li, Y.; Wang, L. J.; Fan, H. L.; Shangguan, J.; Wang, H.; Mi, J. Removal of Sulfur Compounds by a Copper-Based Metal Organic Framework under Ambient Conditions. *Energy Fuels* **2015**, *29*, 298.
(59) Petit, C.; Burress, J.; Bandosz, T. J. The synthesis and characterization of copper-based metal−organic framework/graphite oxide composites. *Carbon* **2011**, *49*, 563.
(60) Erdem, B.; Hunsicker, R. A.; Simmons, G. W.; Sudol, E. D.; Dimonie, V. L.; El-Aasser, M. S. XPS and FTIR Surface Characterization of TiO_2 Particles Used in Polymer Encapsulation. *Langmuir* **2001**, *17*, 2664.
(61) Petit, C.; Levasseur, B.; Mendoza, B.; Bandosz, T. J. Reactive adsorption of acidic gases on MOF/graphite oxide composites. *Microporous Mesoporous Mater.* **2012**, *154*, 107.
(62) Levasseur, B.; Petit, C.; Bandosz, T. J. Reactive Adsorption of NO_2 on Copper-Based Metal−Organic Framework and Graphite Oxide/Metal-Organic Framework Composites. *ACS Appl. Mater. Interfaces* **2010**, *2*, 3606.
(63) Wakita, H.; Tachibana, Y.; Hosaka, M. Removal of dimethyl sulfide and t -butylmercaptan from city gas by adsorption on zeolites. *Microporous Mesoporous Mater.* **2001**, *46*, 237.
(64) del Carmen Gimenez-Lopez, M. C.; Räisänen, M. T.; Chamberlain, T. W.; Weber, U. L.; Lebedeva, M.; Rance, G. A.; Briggs, A. D.; Pettifor, D.; Burlakov, V.; Buck, M.; Khlobystov, A. N. Functionalized fullerenes in self-assembled monolayers. *Langmuir* **2011**, *27*, 10977.
(65) Wang, X. L.; Fan, H. L.; Tian, Z.; He, E. Y.; Li, Y.; Shangguan, J. Adsorptive removal of sulfur compounds using IRMOF-3 at ambient temperature. *Appl. Surf. Sci.* **2014**, *289*, 107.
(66) Zhao, Y.; Shen, B.; Sun, H. Adsorptive removal of dimethyl disulfide from methyl tert-butyl ether using an Ag-exchanged ZSM-5 zeolite. *RSC Adv.* **2016**, *6*, 93086.

DOI: 10.1021/acs.iecr.7b02392
Ind. Eng. Chem. Res. 2017, 56, 9541−9550